RUHUNA JOURNAL OF SCIENCE
Vol 16 (2): 63-78, December 2025
eISSN: 2536-8400
http://doi.org/10.4038/rjs.v16i2.157



Faculty of Science
University of Ruhuna

Evaluation of recovered Carbon black as a sustainable alternative to commercial Carbon black in solid tyre cushion compounds

D.M.D.A. De Zoysa[1], J.C. Jayawarna[2], J.S. Hewage[1] and S.A. Ranaweera [1]*

[1]*Department of Chemistry, Faculty of Science, University of Ruhuna, Matara, Sri Lanka*
[2]*LAUGF Corporation (Rubber) Ltd, Millewa, Horana, Sri Lanka*

*Correspondence: samantharan@chem.ruh.ac.lk, ORCID: https://orcid.org/0000-0001-7275-7115

Received: 15th September 2025, Accepted: 15th December 2025, Published: 30th August 2026

Abstract Pyrolysis is a sustainable solution for waste tyre (WT) management. Recovered carbon black (rCB), is a second highest by-product of tyre pyrolysis process, contains a high amount of carbon, ash and inorganic impurities. In the present study, rCB derived from WTs was upgraded through magnetic separation, ball milling, and purified treating twice with 2M HCl and once with 2M NaOH at 60ºC for one hour using 2 g/mL rCB: leachate ratio to obtain demineralized rCB (drCB). Both raw rCB and drCB were characterized by particle size analysis, proximate and ultimate analyses, TGA, ICP-OES, FT-IR, XRD, and iodine adsorption. The drCB exhibited a substantial reduction in ash content from 22.20% to 3.42 % (by weight) and an increase in carbon content up to 94.41 % (% wt). The upgraded drCB was subsequently incorporated into solid tyre cushion compounds as a partial replacement for commercial carbon black (CCB, N550) to evaluate industrial feasibility. Physico-mechanical properties of the drCB compound demonstrated improved modulus, tear strength, hardness, and other properties such as tensile strength, rebound resilience within the industrial standard limits. These findings confirm the technical feasibility of rCB as a partial replacement of the filler in industrial solid tyre cushion compounds, supporting circular economy concept in the rubber and tyre industry.

Keywords: Acid-base purification, demineralized Carbon black, pyrolysis, waste tyres

1 Introduction

Approximately 370 million tyres are discarded worldwide as waste tyres (WTs) each year (Global Recycling 2025). One approach to extending the service life of tyres is the retreading process (Sienkiewicz *et al*. 2012). However, when retreading is no longer feasible, landfilling becomes the ultimate disposal option (Downard *et al*. 2015). Landfilling of WTs poses significant risks to human health due to fire hazards and the

CC BY NC

long-term emission of toxic substances, which can contaminate air, soil, and water (Shirule and Husain 2015, Gradeall International 2023). In addition, WTs stored in open environments often provide breeding grounds for insects, parasites, and microorganisms (Kalverkamp and Pehlken 2016) which are associated with malaria, dengue fever, and other fatal diseases (Herath *et al*. 2024). To overcome these issues, WTs are often shredded and buried (Karmacharya *et al*. 2016).

Waste tyres can be considered valuable resources, as useful materials such as fuels and chemicals can be recovered from them (Choi *et al.* 2014). In particular, WTs can be converted into chemicals and/or alternative fuels through pyrolysis (Islam *et al*. 2008). Pyrolysis is a thermal decomposition process carried out at high temperatures in the absence of oxygen, during which thermal energy breaks down long polymer chains into smaller molecules (Zabaniotou *et al*. 2014, Kordoghli *et al*. 2015). Pyrolysis of WTs mainly produces three fractions: tyre pyrolysis gas (TPG), tyre pyrolysis oil (TPO), and raw recovered carbon black (rCB). The composition and yield of these pyrolysis products depend on reaction conditions such as temperature, pressure, heating time and rate, and the use of catalysts (Raj *et al*. 2013, Williams 2013, Choi *et al*. 2014, Hu *et al*. 2014). Tyres typically consist of approximately 50 % polymers, 20-25 % carbon black, 15-20 % metals, 1-2 % sulphur, and 1-5 % other additives (% by weight) (Henry 2015). Raw rCB is a carbon-rich solid material generated during the pyrolysis of waste tyres and originates primarily from the carbon black used as reinforcing filler in tyre manufacturing. In addition to carbon black, raw rCB contains all inorganic compounds originally present in tyres, as well as significant amounts of condensed by-products formed during the pyrolysis process. Consequently, the total amount of raw rCB produced exceeds the amount of carbon black initially added during tyre production.

However, raw rCB does not possess adequate properties for direct use as a raw material due to its high levels of inorganic impurities and sulphur-containing by-products. Furthermore, raw rCB exhibits heterogeneous surface characteristics, wide particle size distributions, and rough surface morphology. The chemical composition of raw rCB obtained at different pyrolysis temperatures is given in Table 1 (Henry 2015).

Table 1: Composition of raw recovered carbon black at different pyrolysis temperatures (Henry 2015)

Pyrolysis temperature (°C)	Ultimate analysis (wt%)					Ash content (wt%)					
	C	H	N	S	O	Al	Si	Za	Fe	Cu	Ca
450	83.50	0.90	5.10	1.60	8.90	-	1.69	6.68	0.04	-	0.13
500	85.18	1.15	0.64	2.03	8.41	0.15	0.42	4.10	0.20	-	0.37
550	83.00	1.40	0.40	1.70	13.50	0.13	2.66	4.06	0.54	0.01	-
600	78.50	0.50	0.30	2.40	18.30	0.14	-	3.37	0.38	0.03	0.30

In order to comply with government laws, the end product manufacturing process must be able to properly control the ash content. Approximately three hundred and fifty

kilograms of raw rCB are generated from one ton of discarded tyres. The raw rCB is disposed to the environment, or remain in the pyrolysis plant with no use. Accumulation of rCB will eventually be landfilled, and it is considered as a cost to the pyrolysis plant.

Many sources suggested that rCB could be utilized as carbon black with the appropriate upgrading procedures. Physical methods have been developed for separating rCB materials based on their size, shape, mass, density, or magnetic properties. Different studies have utilized magnetic separation and pulverization to improve the properties of rCB (Alsaleh and Sattler 2014). Steel wires that are not effectively removed during the shredding may be present in rCB. This is something that should not be neglected in industrially applied rCB upgrading operations. Many studies have suggested using powerful magnets to extract steel magnetically. Sulphur and ash content are removed via acid and/or alkali demineralization. The most commonly utilized acids for rCB demineralization are sulphuric acid and, in particular, hydrochloric acid. Other acids such as hydrofluoric acid and nitric acid have also been reported for removing ash from rCB (Antoniou *et al*. 2014) particularly sulphur, and silicon dioxide (Jiang *et al.* 2022, Laithong *et al*. 2025). Various researchers have employed alkali such as KOH and NaOH for rCB demineralization. Both of these bases react with silicon dioxide. Many researchers have employed harsh reaction conditions on lab-scale equipment, such as strong acid/base concentrations, extended extraction durations, or high-volume ratios to remove ash from rCB, which are infeasible on a commercial scale (Henry 2015, Zhang *et al*. 2018).

Commercial Carbon black (CCB) has a wide range of industrial applications as an additive. CCB can be used as a filler in both automotive and non-automotive industries such as conveyor belts, rubber boots, and catalyst support in fuel cells. The majority of carbon black is utilized in rubber-related applications (71% in tyres, 22% in mechanical rubber items). Non-rubber products, such as plastics, inks, and paints, account for the remaining 7% (Precedence Research 2025).

The objective of this study is to upgrade raw rCB generated in pyrolysis plants to be used as alternative filler to CCB in industrial applications utilizing economical upgrading methods. For this purpose, dilute acids and bases with low volumes will be used together with short leaching times at relatively low temperatures for upgrading rCB after magnetic separation and ball milling. The application of upgraded rCB in industrial solid tyre compounds represents a key novelty of this study. The proposed rCB upgrading method is novel within the Sri Lankan context, and its application in solid tyre compounds has not been previously reported in the global literature.

2 Material and Methods

2.1 Materials

Raw rCB was produced by waste tyre pyrolysis process using an industrial pyrolysis plant located in industrial zone Puttalum (Rivoga Pvt Ltd, Sri Lanka). Approximately

6500 kg of cleaned waste passenger car tyres were loaded to the pyrolysis reactor and heated it to 425ºC for approximately 10 hours. After heating was stopped and the reactor was cooled to room temperature over a period of 2-4 hours, raw rCB was collected into industrial bags. The raw rCB yield was 2200 kg. For the purification process, HCl, 37% ACS reagent and NaOH, 97% ACS reagent pellets were used (Merck sigma Aldrich, India).

Rubber compounding, commercial trials, and testing were carried out at the Laugf Corporation (Rubber) Ltd, Millewa, Horana, Sri Lanka. Laugf Corporation (Rubber) Ltd. provided other compounding chemicals including CCB, N550 (i.e. a standard rubber-grade carbon black classified according to ASTM D1765 and is widely used as a CCB in rubber compounds, for comparisons), formulations and machineries.

2.2 Magnetic Separation and Size reduction

After production, the raw rCB was processed through a Magnetic drum separator (MDHH-1) to remove residual ferrous particles. Between 0.1 and 0.2 wt% of magnetic fractions are typically present in the raw rCB. The ball mill, a homemade unit with a capacity of 100 L was loaded with 30 kg of raw rCB and about 30 kg of ceramic balls (1–3 cm in diameter). The milling process was conducted for 72 h at a drum rotation speed of 30 rpm. The ball-milled (rCB(B)) samples were then analysed for agglomerate size distribution.

2.3 Acid-Base demineralization of rCB

After magnetic separation and ball milling, 100 g of raw rCB was placed into a 2 L beaker. Then, 200 mL of 2M HCl was added, and stirred at 200 rpm. The resulting slurry was heated to 60 °C and maintained under continuous stirring at 200 rpm for 1 h at an agitator. The demineralized rCB (drCB) was vacuum-filtered, and washed thoroughly with distilled water until neutral.

In the second purification step, the obtained sample was subjected to a second acid leaching step under same conditions (2M HCl, 60 °C, 200 rpm, 1 h) described in the first step. After the second demineralization, the resultant slurry from second step was transferred to another 2L beaker, 200 mL of 2 M NaOH was added and sample was heated to 60 °C and maintained under continuous stirring at 200 rpm for 1 h. The treated slurry was then vacuum-filtered, washed with distilled water until the filtrate was neutral, and dried at 120°C.

As shown in the schematic flow diagram describing the preparation of samples for industrial trials (Figure 1), the ball-milled sample was subjected to acid-base demineralization, and drCB sample was produced. Two samples were used for both characterizations and rubber compounding tests including drCB, and N550 as the control sample. After demineralization step, the drCB was transferred to a clean glass tray and dried in an oven at 120 °C for 2-3 h before characterization and compounding. Purification steps were repeated few times to obtain minimum 500g of each

demineralized sample, ensuring sufficient material for subsequent rubber compound preparation.

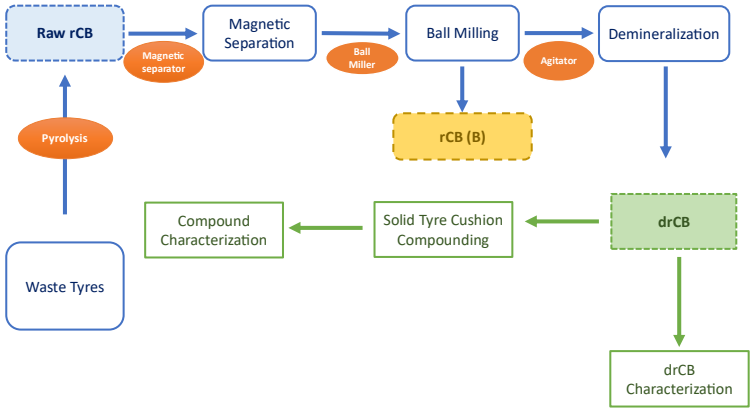


Fig 1: Sample preparation procedure of demineralized recovered Carbon black (drCB)

2.4 Initial characterization of rCB and drCB

Analysis of agglomerate sizes

Particle size of raw rCB and drCB were characterized using a Fritsch Analysette 22 Nano Tech particle size analyser. The measuring range was 0.08 µm to 2100 µm, and the analysis was performed using the wet method.

Ultimate and proximate analyses

PerkinElmer® 2400 Series II CHNS/O Elemental Analyzer (2400 Series II) was used to analyse the percentages of carbon (C), hydrogen (H), sulfur (S), and (N) nitrogen content of the rCB and N550 samples. The moisture, ash and volatile matter contents were determined by ASTM D2867, ASTM D2584 and ASTM D2369 respectively. The fixed carbon content was calculated by subtracting moisture (%), volatile matter (%), and ash (%) from 100%.

Thermogravimetric Analysis (TGA)

PerkinElmer TGA 4000 was used to determine the thermal decomposition data for all samples. An amount of 5-10 mg of CB sample was placed on the sample holder maximizing the surface area of the sample in TGA pan and the samples were first heated to 50 °C and held at 1 minute under a N_2 flow rate of 20 mL/min. The sample was then heated from 50 °C to 900 °C at 20 °C/min and stabilized at 900 °C for 1 min. Following this, the N_2 was replaced with O_2 (20 mL/min) at 550 ^{0}C.

Inductively Couple Plasma-Optical Emission Spectroscopy (ICP-OES) Analysis

The metal elements in the samples were determined using a Perkin Elmer Avio 200 ICP-OES system, equipped with a Scott spray chamber and a cross-flow nebulizer, following the ISO 19050 method.

Textural characterization

The iodine absorption number was determined using the ASTM D 4607 method. This test method is based upon a three-point adsorption isotherm. A standard iodine solution is treated with three different weights of activated carbon under specified conditions. The carbon treated solutions are filtered to separate the carbon from the treated iodine solution (filtrate). Iodine remaining in the filtrate is measured by titration. The amount of iodine removed (per gram of carbon) is determined for each carbon dosage and the resulting data were used to plot an adsorption isotherm. The amount of iodine adsorbed (mg per gram of carbon) at a residual iodine concentration of 0.02 N is reported as the iodine number.

X-ray diffraction (XRD)

The XRD analyses were conducted using a Bruker D8 Focus X-ray diffractometer with Cu-Kα radiation (λ = 1.54 Å) operated at 40 kV. Samples were scanned over a 2θ range of 5° to 80° at a scan rate of 4°/min.

2.5 Preparation and evaluation of physico-mechanical properties

Rubber compounds were prepared according to the control formula of Laugf Corporation (Rubber) Ltd for solid tyre cushion compounds as summarized in Table 2. All ingredients were accurately weighed and incorporated following the mixing cycle specified in Table 3 and 4. Compounding was carried out in a XM-160 × 30C Banbury mixer operated at 150-160 °C and 30 rpm at the bar pressure of five. Upon completion of the first stage mixing, the compound was transferred to a Kneader mixer (Model X(S)N 110/30) with a rotter speed of 30 rpm at 15 bar pressure. Sulphur was added to the compound in Kneader mixer and mixing was limited for 2.5 minutes while controlling the temperature around 70-100 ^{0}C.

After completion of the second stage, the compound was sheeted out through a two-roll mill (Model: XK 550) with a roller speed of 22.5 m min^{-1} and prepared compounds were kept for more than 16 hours at room temperature (< 25 ^{0}C) before initiate the curing process. Cure properties were evaluated using a EKT-100H oscillating disk rheometer following the ATM D 5289/2084 standard. The sample of the uncured compound (5g) was placed on the preheated rotor, and the heated top die cavity was immediately lowered onto the lower die, ensuring the cavity was fully filled. The sample was cured at 150 °C for 30 min.

Table 2. Cushion compounds formula

Ingredients	Control Sample (phr)	drCB (B) H2S1 Sample (phr)
Elastomer	100	100
Reclaim Rubber (Superfine)	10	10
Reinforcing Filler	50	30
Mineral Filler	80	80
rCB	0	20
Stearic Acid	2	2
ZnO (99.5%)	4.5	4.5
Antioxidant 1	1	1
Antioxidant 2	1	1
Antiozonate	1	1
Vulcanizing Agent	1	1
Primary Accelerator	1.25	1.25
Secondary Accelerator	0.2	0.2
Pre Vulcanization Inhibitor	0.2	0.2
Total	252.15	252.15

Table 3. Mixing cycle of Stage 1 compound

Ingredients	Milling time (seconds)
Elastomer + Reclaim Rubber	0
½ Reinforcing Filler + ½ Mineral Filler	90
½ Reinforcing Filler + ½ Mineral Filler + Chemicals	90
Ram Sweep	90
Dump	35-50

Table 4. Stage 2 mixing cycle

Ingredients	Milling time (seconds)
1st Stage Compound	0
Chemical	30
Clean	45
Dump	75

Specific Gravity (SG)

SG was measured using the SHIMADZU UX420S direct reading specific gravity balance, according to the method of ASTM D792. The SG scale was printed on the vertical plate, and a pointer attached to a beam pivoted on fine bearings register with the scale. The test was carried out under the temperature of 25 ℃ using 5-12 g weighted test pieces. The test piece was suspended on a needle from an arm at one end of the beam which is zeroed by means of quickly adjustable sliding weights. Then test piece was immersed in water contained in a glass beaker located on a friction-clamped platform. The platform can be raised and lowered easily and remains in position without any additional clamping. When the test piece was immersed the pointer read directly in SG. The average properties were calculated after taking the statistical value of three measurements for each compound.

$$\text{Specific Gravity} = \frac{\text{Density of Sample}}{\text{Density of Water}}$$

Tensile strength

Dumbbell-shaped test specimens were prepared from a compression-moulded sheet with a thickness of 1.2 mm. Five test specimens were cut using a die cutter and fixed in an eccentric roller grip. Tensile testing was conducted using GT-7010-AEP tensometer at a strain rate of 500 mm/min, following the ASTM D 412 test method. The test was performed at 25 °C. The average tensile strength was calculated (n= 3-5 specimens). From the stress-strain curve, key mechanical properties were determined, including tensile strength, elongation at break, and modulus at 300% elongation.

Tear strength

Crescent-shaped test specimens were prepared from a compression-moulded sheet with a thickness of 1.2 mm. Tear testing was performed using a GT-7010-AEP tensometer at a constant traverse rate of 500 mm/min, following the ASTM D 624 test method at 25 °C. The average tear strength was calculated from five test specimens.

Hardness

The hardness was measured using Shore-A-durometer (Model: SHR-A-Gold) according to ASTM D 2240 standard. Test specimens of size 50 mm x 50 mm were punched from a post-cured sheet and kept at 27 ºC for 24 h prior to testing. Samples were placed on a rigid surface with the sole side at facing up. Pressure was applied slowly to the test specimen and maximum pressure was reached within 3 to 4 seconds. The hardness value was measured in three places and the average value was taken as the hardness.

Rebound Resilience

The rebound resilience test was carried out in accordance with the ASTM D 2632 test method. In this method, a plunger suspended from a given height above the specimen was released and the rebound height was measured. The resilience scale was marked in 100 equally spaced divisions and hence the rebound height was equal to the resilience percentage. The hardness test button was used as the test piece for the rebound resilience. Three test pieces were used from one compound and average values were obtained as the means of resilience. The rebound resilience test was carried out at room temperature of 25 ℃.

2.6 Statistical analysis

Statistical analysis was performed using one-way analysis of variance (ANOVA) to evaluate differences in specific gravity, tensile strength, elongation at break, tear strength, hardness, modulus at 300% and rebound resilience among three groups: the control sample (N550), raw rCB, and drCB. Before performing ANOVA, the normality of the model residuals was assessed using the Shapiro–Wilk test, while the homogeneity of variances was evaluated using Levene's test. For parameters that did not satisfy the normality assumption, an inverse transformation was applied, and the

assumptions were reassessed using the transformed data. One-way ANOVA was then conducted to determine whether statistically significant differences existed among the group means. When a significant difference was identified, Tukey's honestly significant difference (HSD) post-hoc test was performed to identify differences between individual pairs of groups. Statistical significance was considered at a 5% significance level ($p < 0.05$).

3 Results and Discussion

3.1 Agglomerate size

Agglomerate size of the raw rCB was obsereved between 137.735 to 554.61 µm (Figure 2). The agglomerate size of rCB was significantly reduced to 0.850–19.557 µm, with a D50 of 10.155 ± 2.965 µm after ball milling, which was close to ideal range for rubber compounding (Wang *et al*. 2019, Zhang and Li 2021). The significant reduction in agglomerate size improves the specific surface area, enhancing filler interaction in the rubber matrix and dispersion uniformity (Liu *et al*. 2020).

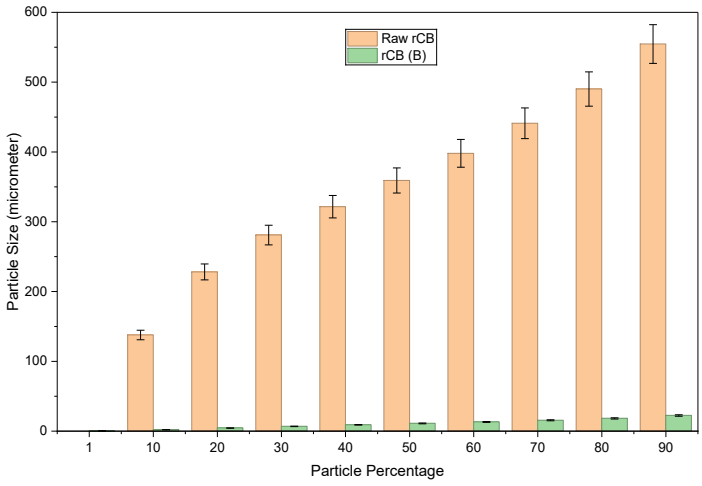


Fig 2. Particle Size distribution of recovered carbon black (rCB) samples

3.2 Ultimate and proximate analysis

As shown by the contents of C, H, N and S for all samples (Table 5), there is a clear increment of carbon content after demineralization. A maximum carbon content of 94.41 wt% was found in drCB. This represents an increase of approximately 30 wt% compared to the raw rCB and confirms the strong leaching efficiency of HCl in generating H^+ ions for effective impurity removal. As expected, the ash content of rCB gradually decreased with sequential washing using HCl and NaOH, reaching a final

value of 3.42 wt% for drCB. The fixed carbon content steadily increased as acid and base leaching removed inorganic impurities while preserving carbon.

Table 5: Characterization of rCB and the standard N550

Analysis	Raw rCB	rCB(B)	drCB	N550
Proximate analysis (wt %)				
Ash	22.20	17.71	3.42	≤0.75
Volatile Matter	14.23	11.30	3.81	n.r
Moisture Content	2.35	2.31	1.44	n.r
Fixed Carbon	61.22	68.68	91.33	95.71
Ultimate analysis (wt %)				
Carbon	65.03	69.39	94.41	98.90
Hydrogen	0.27	0.49	0.56	0.28
Nitrogen	0.21	0.14	0.21	0.30
Sulfur	3.12	2.43	2.50	0.56
ICP- OES Analysis (wt%)				
Zn	1.14	1.12	0.36	n.r
Fe	0.34	0.30	0.10	n.r
Mg	0.25	0.20	0.04	n.r
Cu	0.02	0.02	0.01	n.r
Ca	2.71	2.68	0.07	n.r
Textural Analysis				
Iodine number (mg/g)	38.69	120.75	92.54	43.00

n.r – not reported

3.3 TGA

Figure 3 shows the TGA profiles of rCB, drCB and N550 based on single samples. As observed, all samples show a very small weight loss before 400 ºC related to moisture released in accordance to the proximate analysis results. Between 400 ºC and 550 ºC, all the rCB samples show the beginning of an apparent weight change related to the volatile content released and N550 sample exhibited considerable weight loss after 600 ºC. The decomposition pattern of N550 shows higher total weight loss than other sample, reflecting lower ash contents of ≤ 0.75 wt% and agrees well with the proximate analyses data. These findings are further supported by ICP-OES data (Table 5).

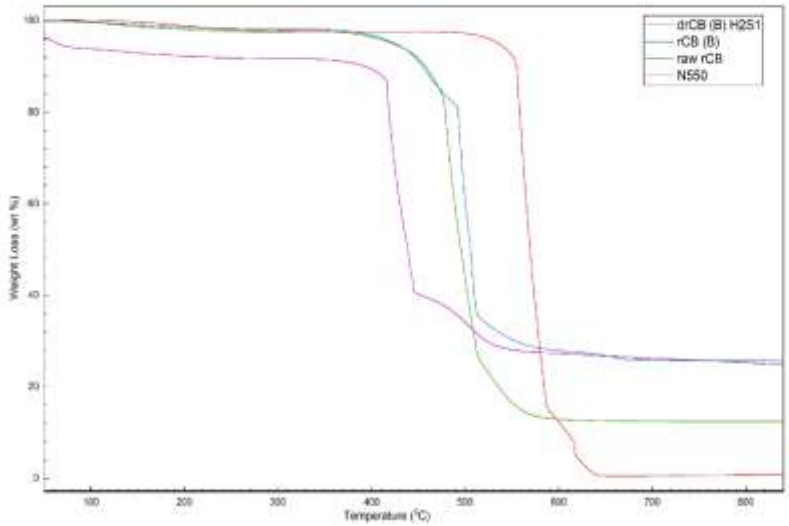


Fig. 3: Thermogravimetric Analysis (TGA) Profiles of rCB samples

3.4 ICP-OES

Inorganic contaminants such as Zn, Mg, Fe, Cu, and Ca were effectively removed through sequential acid and base treatments. Additionally, successive HCl washes selectively extracted both inter- and intra-particle impurities, contributing to a reduction in particle size (Anupabphan *et al*. 2025). Subsequent HCl and NaOH washings of rCB(B) minimized these impurities lowering Zn to 0.36%, Fe to 0.10%, Mg to 0.04%, and Ca to 0.07%. The overall ash content of rCB reduced to 3.42 wt% in the most refined drCB sample (as determined by TGA), representing an approximately 82% reduction from the initial ash content of raw rCB.

3.5 Textural characterization

The drCB sample shows improved iodine absorption values compared to the raw rCB which implies that ball milling has impact on surface area (Table 5). A significant increase in iodine absorption was observed after demineralization, with value reaching 92.54 mg/g for drCB.

3.6 XRD

XRD analyses used for identify metallic crystallites on rCB surfaces. The XRD patterns of rCB samples and N550 are shown in Figure 4. The primary crystalline features observed in XRD include graphite-like crystallites and metallic sulfides. After ball milling, the rCB(B) sample displays several intense peaks at 2θ values of 29°, 30°,

and 47° corresponding to ZnS crystallites. Additionally, less intense peaks at ~30°, ~36°, and ~40° strongly match ZnO.

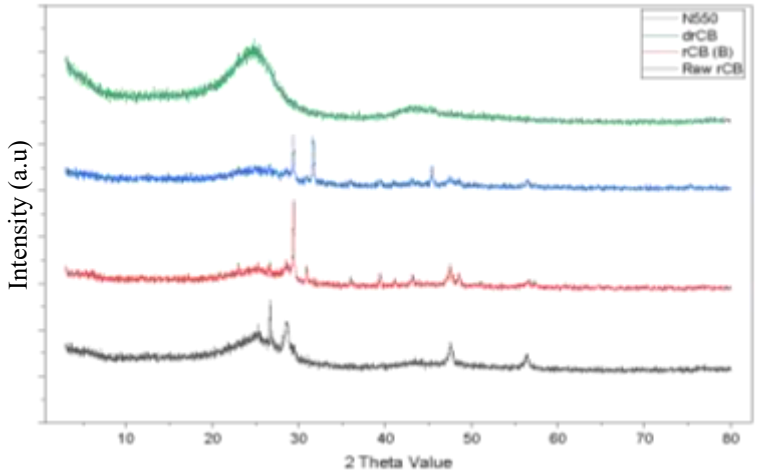


Fig. 4: X-ray diffraction Analysis

Notably, the number and intensity of XRD peaks of ball-milled rCB are higher than those of drCB, providing strong evidence for the release of intra- and inter-particulate contaminants. However, with sequential washing, peak height and area decreased in drCB diffractogram, indicating the removal of metallic impurities in soluble form.

3.7 Evaluation of physico-mechanical properties of tyre cushion compounds

Since purity of raw rCB and ball milled rCB was poor, only drCB was used to prepare rubber compounds together with N550. Physico-mechanical properties of N550 and drCB incorporated solid tyre cushion vulcanizates have been reported in Table 6 along with the acceptable standard levels of properties of solid tyre cushion compounds. According to the formula listed in Table 2, drCB compound was prepared altering 20 phr of reinforcing filler in the control formula. This partial replacement is beneficial for improve the filler-rubber matrix interactions while improving the reinforcement of the compound.

Specific Gravity (SG)

The SG of tyre compounds is crucial when optimizing the amount of compounds used to fill the tyre mould, ensuring proper filling without wasting the rubber compounds. The SG of tyre vulcanizates showed no statistically significant difference among the three samples at 5% significance level.

Table 6: Physico-mechanical properties of solid tyre cushion compounds

Parameter	Standard Limit	Control N550	Raw rCB	drCB	Test Method
Specific Gravity	1.36 ± 0.02	1.37	1.41	1.40	ASTM D 792
Tensile Strength (MPa)	13.70 - 18.60	16.30	6.88	15.30	ASTM D 412
Elongation at break (%)	420 - 500	483.00	243.00	423.00	ASTM D 412
Modulus at 300% (MPa)	8.33 - 11.78	8.53	-	10.10	ASTM D 412
Tear Strength (MPa)	-	3.92	3.85	4.01	ASTM D 624
Hardness (Shore °A)	63 - 69	67.00	68.00	70.00	ASTM D 2240
Rebound Resilience (%)	-	58.00	50.00	51.00	ASTM D 2632

Tensile strength, elongation at break (EB) and Modulus at 300%

The tensile strength value of drCB was within the standard limit which is required for solid tyre cushion compounds but slightly lower than that of the control sample. Tensile strength of the treated sample increased significantly after the demineralization of raw RCB ($p<0.05$). The EB can be used to study the reinforcement of rubber vulcanizates as an effective tool (Ajam *et al*. 2016), and EB of drCB is within the standard limits and improved EB compared to the raw rCB.

A 300% modulus value indicates a material stiffness at a 300 % elongation. Higher modulus means hard material and lower modulus mean flexible material (Norman, n.d). The modulus value of drCB was within the standard limit which required for solid tyre cushion compounds but higher than the control sample. These results attributed to the reinforcement of added by drCB into the compounds and these compounds comply with the standard limits of the cushion compounds.

Tear Strength

Tear strength represents the resistance to initiate a crack and the energy required to propagate the crack (Gunasekara *et al*. 2019). According to the results, vulcanizates showed no statistically significant difference among the three samples at 5% significance level.

Hardness

The hardness (Shore A) of compounds showed no statistically significant difference among the three samples at 5% significance level. Also, the hardness of drCB vulcanizate was slightly higher than the accepted standard limit of 36-69 Shore A. The reason for the slight increment of hardness may be due to combined effect of the drCB and CB fillers for the reinforcement (Bijarimi *et al.* 2010a).

Rebound Resilience

Rebound resilience of the drCB has decreased compared to control sample and showed no statistically significant difference between raw rCB and drCB samples at 5% significance level. This behavior could be observed due to improvement of hardness

and specific gravity, which indicate the high reinforcement and packing of rubber in the vulcanizates (Bijarimi *et al*. 2010b). However, other properties have indicated the values within the specification range showing that the applicability of rCB in solid tyre cushion compounds.

4 Conclusions

This research investigated the industrial applicability of upgraded drCB derived from waste tyres, specifically in solid tyre cushion compounds. The combined treatments of magnetic separation, ball milling, and sequential acid-base demineralization proved highly effective in reducing ash and inorganic contaminants while significantly enhancing the carbon content from ~ 65% to ~ 94% and surface characteristics of drCB. The upgraded drCB sample achieved an ash reduction of approximately 82% and exhibited improved textural properties, as evidenced by increased iodine adsorption values.

When incorporated into industrial solid tyre cushion compounds as a partial replacement for N550 filler, the upgraded rCB exhibited physico-mechanical properties that improved or closely matched with industrial specifications. Although slight improvements were observed in hardness and rebound resilience, other properties including tensile strength, elongation at break, modulus, and tear resistance confirmed the reinforcing capability of the treated rCB. These results indicate strong filler–rubber interactions and effective dispersion within the rubber matrix of drCB.

Overall, the findings highlight the potential of upgraded rCB as a viable, value-added alternative to conventional fillers in solid tyre applications. Real world applications are limited in rCB, due to lack of evidence-based research and findings. The proposed upgrading methodology offers a practical and scalable solution for sustainable material reuse within the tyre manufacturing industry.

Acknowledgements

Authors greatly acknowledge the financial support given by AHEAD RIC Round 2 Number 18 grant, and the comments from RJS reviewers.

References

Ajam AM, Al-Nesrawy, SH, Al-Maamori M. 2016. Effect of reclaim rubber loading on the mechanical properties of SBR composites. *International Journal of Chemical Sciences* 14(4): 2439-2449.

Alsaleh A, Sattler ML. 2014. Waste tire pyrolysis: influential parameters and product properties. *Current Sustainable/Renewable Energy Reports* 1(4): 129-135.

Antoniou N, Stavropoulos G, Zabaniotou A. 2014. Activation of end-of-life tyres pyrolytic char for enhancing viability of pyrolysis–Critical review, analysis and recommendations for a hybrid dual system. *Renewable and sustainable energy reviews* 39: 1053-1073.

Anupabphan T, Narischat N, Theinnoi K, Hartley UW, Wongkhorsub C. 2025. Chemical process enhancement of pyrolytic carbon black from waste tires. *ACS omega* 10(37): 42451-42460.

ASTM D4607-14. 2014. Standard test method for determination of iodine number of activated carbon. *Annual Book of ASTM Standard Test Method*. ASTM International.

Bijarimi M, Zulkafli H, Beg MDH. 2010a. Mechanical properties of industrial tyre rubber compounds. *Journal of Applied Sciences (Faisalabad)* 10(13): 1345-1348.

Bijarimi Mohd, Zulkafli Hassan, M, Dalour Beg, Zainal Abidin. 2010b. The Effect of Carbon Black Grades in Tyre Tread Compound. *Journal of Engineering and Technology* 1: 73-82.

Choi GG, Jung SH, Oh SJ, Kim JS. 2014. Total utilization of waste tire rubber through pyrolysis to obtain oils and CO_2 activation of pyrolysis char. *Fuel* 120: 66–73.

Dick DT, Agboola O, Ayeni AO. 2020. Pyrolysis of waste tyre for high-quality fuel products: A review. *AIMS Energy* 8(5): 869-895.

Downard J, Singh A, Bullard R, Jayarathne T, Rathnayake CM, Simmons DL, Wels BR, Spak SN, Peters T, Beardsley D, Stanier CO. 2015. Uncontrolled combustion of shredded tires in a landfill–Part 1: Characterization of gaseous and particulate emissions. *Atmospheric Environment* 104: 195-204.

Global Recycling (n.d.). Magazine. Available at: https://global-recycling.info/magazine (Accessed: 16 January 2026).

Goksal FP. 2022. An economic analysis of scrap tire pyrolysis, potential and new opportunities. *Heliyon* 8(11): e11669

Gradeall International. 2023. Risks of burning tires and tire recycling alternatives. Available at: https://gradeall.com/risks-of-burning-tires-and-tire-recycling-alternatives/ (Accessed: 16 January 2026).

Gunasekara TDIK, Ranatunga RRMSK, Wijesinghe HGIM, Senevirathna AMWK. 2019. A dual filler system for low-speed tire base compound. *Journal of Technology and Value Addition* 1 (2): 17-30

Han W, Han D, Chen H. 2023. Pyrolysis of waste tires: a review. *Polymers* 15(7): 1604.

Henry KL. 2015. Upgrading pyrolytic tyre char through acid-alkali demineralisation (Master dissertation, Stellenbosch: Stellenbosch University).

Herath JMK, De Silva WPP, Weeraratne TC, Karunaratne SP. 2024. Breeding habitat preference of the dengue vector mosquitoes *Aedes aegypti* and *Aedes albopictus* from urban, semiurban, and rural areas in Kurunegala District, Sri Lanka. *Journal of Tropical Medicine* 2024(1): 4123543.

Hu H, Fang Y, Liu H, Yu R, Luo G, Liu W, Li A, Yao H. 2014. The fate of sulfur during rapid pyrolysis of scrap tires. *Chemosphere* 97: 102-107.

Islam MR, Haniu H, Beg MRA. 2008. Liquid fuels and chemicals from pyrolysis of motorcycle tire waste: product yields, compositions and related properties. *Fuel* 87 (13-14): 3112-3122.

Jiang G, Pan J, Deng W, Sun Y, Guo J, Che K, Zhang T. 2022. Recovery of high pure pyrolytic carbon black from waste tires by dual acid treatment. *Journal of Cleaner Production* 374: 133893.

Kalverkamp M, Pehlken A. 2016. Support for improved scrap tire re-use and Recycling Decisions. In Information Technology in Environmental Engineering: *Proceedings of the 7th International Conference on Information Technologies in Environmental Engineering*: 41-52.

Kordoghli S, Paraschiv M, Tazerout M, Zagrouba F. 2015. Waste tyres pyrolysis: Managing the environmental hazards of scrap tyres. In*: the Sixth international Renewable Energy Congress*: 1-6

Laithong T, Nampitch T, Ourapeepon P, Phetyim N. 2025. Quality improvement of recycled carbon black from waste tire pyrolysis for replacing carbon black N330. *Scientific Reports* 15(1): 23726.

Martínez JD, Puy N, Murillo R, García T, Navarro MV, Mastral AM. 2013. Waste tyre pyrolysis–A review. *Renewable and sustainable energy reviews* 23: 179-213.

Norman DT. (Web article). Rubber grade carbon blacks. Available at: http://www.continentalcarbon.com/pdfs/what_is_carbon_black.pdf (Accessed: 16 January 2026).

Precedence Research. 2025. Carbon Black Market Size, Share, and Trends 2025 to 2034. Available at: https://www.precedenceresearch.com/carbon-black-market (Accessed: 16 January 2026).

Raj RE, Kennedy ZR, Pillai BC. 2013. Optimization of process parameters in flash pyrolysis of waste tyres to liquid and gaseous fuel in a fluidized bed reactor. *Energy conversion and Management* 67: 145-151.

Shankar S, Gadi R, Sharma SK, Mandal TK. 2022. Identification of carbonaceous species and FTIR profiling of $PM_{2.5}$ aerosols for source estimation in old Delhi region of India. *MAPAN* 37(3): 529-44. doi: 10.1007/s12647-022-00575-0.

Shirule PA, Husain M. 2015. Reuse of scrap tyre as partial replacement of fine aggregate in concrete and its impact on properties of concrete. *International Journal of Civil & Structural Engineering* 5(4): 353-359.

Sienkiewicz M, Kucinska-Lipka J, Janik H. Balas A. 2012. Progress in used tyres management in the European Union: A review. *Waste Management* 32(8): 1742–1751.

Williams PT. 2013. Pyrolysis of waste tyres: A review. *Waste Management* 33(8):1714-1728.

Wu Q, Zhang Q, Chen X, Song G, Xiao J. 2022. Integrated assessment of waste tire pyrolysis and upgrading pathways for production of high-value products. *ACS Omega* 7(35): 30954–30966.

Xia R, Wang W, Fu Z, Guo Y, Liu H, Zhang Q, Wang G, Wang N, Tao Z, Wang X. 2025. Molecular Characterization of Waste Tire Pyrolysis Oil: 14C Distribution and Potential for Sustainable Fuels and Chemicals. *Energy & Fuels* 39(17): 8107-8119.

Zabaniotou A, Antoniou N, Bruton G. 2014. Analysis of good practices, barriers and drivers for ELTs pyrolysis industrial application. *Waste management* 34(11): 2335-2346.

Zhang X, Li H, Cao Q, Jin LE, Wang F. 2018. Upgrading pyrolytic residue from waste tires to commercial carbon black. *Waste Management & Research* 36(5): 436-444.